Hindawi
Wireless Communications and Mobile Computing
Volume 2022, Article ID 5968207, 12 pages
https://doi.org/10.1155/2022/5968207

Research Article

Research on Embedded Ball Screw Diagnosis System for Mechanical Fault Based on Bispectral Image

Da Lv,[1,2] Chao Zhang,[1] Wentao Zhao,[1] and Shuai Wang[1]

[1]*College of Mechanical Engineering, Inner Mongolia University of Science and Technology, Baotou, 014030 Inner Mongolia, China*
[2]*Baotou Vocational & Technical College, Baotou, 014030 Inner Mongolia, China*

Correspondence should be addressed to Chao Zhang; zhanghero@imust.edu.cn

Received 10 June 2022; Revised 21 July 2022; Accepted 28 July 2022; Published 28 September 2022

Academic Editor: Chia-Huei Wu

Ball screw is one of the main basic transmission components in CNC machine tool feed system because of its high transmission efficiency, positioning accuracy, and rigidity. It plays an irreplaceable role in the process of machine tool torque transmission and positioning. However, ball screw is also one of the parts which are easy to break down in the feed system. If it breaks down, it will affect the processing accuracy of the whole machine tool and even cause shutdown. Numerical control means that digital control is a high-efficiency technology that uses digital information to control mechanical movement and processing processes. Therefore, to increase the high-speed and high-precision operation ability of CNC machine tools, research and development of efficient and reliable predictive maintenance and issue identification technology to guide maintenance of CNC machine tools are critical. Throughout this study, a bispectrum image-based embedded defect fight against the disease for cylindrical gears is provided. Firstly, the bispectrum of fault signal is generated by Wavelet Packet Threshold denoising, wavelet packet reconstruction, and bispectrum analysis, and the characteristics of bispectrum are represented by the first kind of gray moments. These feature statistics are used as input feature vectors of BP neural network pattern recognition algorithm to classify these feature sets and identify the corresponding gear fault types. Experiments show that under the condition of noise, after 14.5 hours of testing, the NGI has increased significantly and can be used to diagnose faults in the gear system, and the method achieves relatively ideal recognition rate and verifies the feasibility of gear box fault diagnosis method based on image recognition. The code compiled by OpenCV library is easy to transplant to embedded system, with high development efficiency and reliable program operation. OpenCV has the characteristics of powerful matrix computing capability and convenient and flexible interface, and it is a general algorithm that can realize real-time image processing.

1. Introduction

Ball screw pair was born in the early 20th century. Because of the complexity of its manufacturing process, it has not been popularized for a long time. General Motors is the first company to use ball screw pairs innovatively as automotive technology [1, 2] and to make reasonable arrangements for automotive steering parts. In the 1940s, the United States produced a large number of ball screw pairs. Three years later, the first application of ball screw pairs was carried out on aircraft. The development of precision screw grinder has greatly promoted the further improvement of ball screw pair technology. Along with the development of a large number of electrical industry, it also affects the research and development of ball screw pair. After 1950, ball screw pairs began to be popularized in most countries. Some companies are the main producers [3–5]: ROTAX Company in Britain, NK Company in Japan, and so on. China began to study ball screw pairs around 1960. After half a century of development, domestic ball screw pairs have achieved great success with a certain scale, but there is still a big gap between them and developed countries, although there are many domestic manufacturers. However, the technology is uneven; most of them belong to the initial stage and small production stage. For some large manufacturers, their output is very small. Moreover, the quality of production cannot match with the mechanical products [6, 7].

The components of ball screw pair are screw, nut, ball, and reverser. The ball is in the spiral groove and clamped

between the screw and the nut. As a rolling element, it constitutes a complete ball chain reciprocating system [8]. While the screw rod rotates continuously, the ball moves at the same time. Its track is the thread of the nut, and the movement of the ball is not only rotating relative to the screw rod but also rotating to itself. From such a motion system, we can know that there is resistance caused by contact between different balls and between balls and nuts [9]. The guide devices such as reversers are installed at the ends of nuts to avoid the ball from accidentally leaving its track in the course of movement. The guide device and the thread of the nut constitute a closed loop, so the ball rolls repeatedly on its orbit with rotation [10]. Ball screw is one of the important components in the precision technology industry and precision machinery industry. It has the characteristics of high positioning accuracy and low pollution. Ball screw has become one of the important components in the positioning and measurement system of the precision technology industry and precision machinery industry recently.

At present, there is a big gap in the production level and quality of ball screw pairs at home and abroad, such as speed and accuracy can fully reflect [11, 12]. At present, the speed and acceleration of domestic ball screw pairs are more than half of the distance from abroad. The globalization of economic development and the rapid development of technology have resulted in the vigorous development of machinery manufacturing industry in today's society. Ball screw pair is a necessary part of some electrical and automation machinery, so the development of ball screw pair restricts the development of mechanical manufacturing. At present, due to the development of polar linear motor in order to achieve maximum speed, but due to the production process is too complex and high cost, it has not been promoted [13]. This prompted the ball screw pair to make more efforts in speed drive to meet the requirements of social and mechanical progress [14].

Due to the recent development of machinery in full swing, the speed has increased nearly three times, reaching the high speed of development [15]. Such a rapid development has great advantages: in a fixed period of time, the processing speed of materials can be increased by about five times, which is conducive to the current high-speed processing; The processed parts will not generate excessive heat due to high-speed operation [16]; parts can be made more precise and cleaner by high-speed processing technology; the residual pressure on the surface of the processed devices will be much smaller [17]. Because of the high-speed level and obvious advantages of this kind of processing objects, the development of this technology has attracted sustained international attention, especially in the American aerospace industry, which has been widely applied. At present, such technology can be seen in various automobile manufacturing and mechanical production. The development of high-speed machining technology has put forward higher requirements for high-speed manufacturing of ball screw pairs. Ball screw pair to achieve high speed is to increase its lead and rotation speed and to solve these problems is facing great challenges [18, 19]. The guide of ball screw pair is determined by its diameter, so we must consider the relationship between the diameter and the lead to solve it. If we blindly increase the lead, it will also bring some side effects [20], so we must find the equilibrium state. The speed of the ball screw pair is determined by the critical resonance speed NC, which is related to the material and product specifications of the screw rod. The DN value is used to identify the critical safe speed of ball movement in thread trajectory and reverse trajectory. D is the diameter of the screw rod, and N is the speed of the screw rod. In order to make the speed faster [21, 22], it is necessary to study the design of threads and the reverse device more carefully, to improve the bearing's compressive resistance, and to require more stringent accuracy, so as to improve the DN value [23]. Attention should be paid to the noise caused by high-speed operation and the increase of temperature. Reasonable solutions to the problems described will effectively improve the current high-speed development of ball screw pairs. In order to achieve rapid development, we can adopt some convenient methods, such as reasonable replacement of some parts of the screw pair, ball, and nut, so as to achieve the optimization and upgrading of the overall level of the object [24]. Of course, these measures must be supported by real experimental data. In order to achieve the real experimental test [25], first of all, a reasonable test method must be established and a unified standard should be applied to the dynamic test of ball screw pairs [26, 27]. It is necessary to combine theory with practice so as to make innovative devices with real theoretical basis. Nowadays, Gangang is starting in this field in China. It is necessary to learn and explore advanced technology from abroad. Therefore, in the future, through the development of mechanization, the ball screw will realize the development of high precision and high efficiency, which can improve the production efficiency of CNC machine tools.

Because of its high transmission efficiency, positioning accuracy, and stiffness, ball screw pair has become one of the main basic transmission components in the feed system of NC machine tools. It plays an irreplaceable role in the moment transmission of machine tools and in the process of processing and positioning. When the ball screw pair fails, it will directly affect the normal work of CNC machine tools. Therefore, theoretical and experimental research on mechanism analysis, condition monitoring method, state signal acquisition, processing, feature extraction and screening, model establishment, fault identification, and diagnosis of typical faults of ball screw pairs of machine tools are carried out. Developing an efficient and reliable condition monitoring and fault diagnosis system for ball screw pairs of NC machine tools is of great significance to ensure the high-speed and high-precision operation ability of NC machine tools, the processing accuracy of parts, and improving the production efficiency of machine tools. The dual-spectral image is to realize the registration of ultraviolet-infrared dual-spectral images, which can provide strong technical support for the current ultraviolet-infrared dual-spectral detection field.

In this paper, an embedded fault diagnosis method based on bispectrum image is proposed for cylindrical gears. Firstly, the bispectrum of fault signal is generated by Wavelet

Packet Threshold denoising, wavelet packet reconstruction, and bispectrum analysis, and the characteristics of bispectrum are characterized by the first kind of gray moments. These feature statistics are used as input feature vectors of BP neural network pattern recognition algorithm, and then these feature sets are classified to identify the corresponding gear fault type. Experiments show that under the condition of noise, the method achieves relatively ideal recognition rate and verifies the feasibility of gear box fault diagnosis method based on image recognition. The code compiled by OpenCV library is easy to transplant to embedded system, with high development efficiency and reliable program operation. The samples are extracted every 40 minutes, and the signal features can be correctly extracted when SNR =0.

2. Proposed Method

2.1. Wavelet Decomposition and Reconstruction. The characteristic of wavelet analysis is that the size of the window is fixed and the shape is variable. It can analyze localized signal. Its time resolution and frequency resolution can be adjusted automatically according to the signal frequency. Wavelet analysis has developed rapidly in recent years, which is of great significance and widely used. Wavelet analysis can represent the local characteristics of the signal, which is suitable for observing the transient abnormal signal and analyzing its components, so it is called the analysis signal microscope. Wavelet can be used for multi-resolution analysis. At many scales, motions as well as pictures can all be fragmented. After denoising, the denoised signals or images can be obtained by inverse transformation. It has been proved in many fields that the performance of wavelet analysis is better than that of Fourier transform in the processing of non-stationary signals and images. So, in a very short time after the emergence of wavelet analysis, good application results have been achieved in radar signal analysis, fault diagnosis, speech segmentation and synthesis, signal information processing, geophysical exploration, image processing, and other fields.

Let $x(t)$ be a finite energy function, that is $x(t) \in L^2(R)$, its wavelet transform function is:

$$\mathrm{w}_x(a, b\,; \varphi) = \int_{-\infty}^{\infty} x(t)\varphi_{a,b}(t)dt, a > 0. \tag{1}$$

$\varphi_{a,b}(t)$ is the basic wavelet functions are translated and scaled to obtain:

$$\varphi_{a,b}(t) = \mathrm{a}^{-1/2}\psi\left(\frac{t-b}{a}\right). \tag{2}$$

In the formula: b - positioning parameter; a >0 is scale parameter. The $a^{-1/2}$ factor is a normalized constant, so that the energy remains unchanged before and after the transformation. The Fourier substring spectral expression is just as shown in:

$$\overset{\Lambda}{\psi}_{a,b}(\omega) = \mathrm{a}^{1/2}\overset{\Lambda}{\psi}_{a,b}(\mathrm{a}\omega). \tag{3}$$

Wavelet transform is a new transform analysis method. It inherits and develops the idea of localization of short-time Fourier transform, and at the same time overcomes the shortcomings of window size not changing with frequency. When the scale parameters become smaller, the time domain resolution becomes higher, and the corresponding frequency domain resolution is very low. When the scale parameters become larger, the frequency domain resolution becomes higher and the corresponding time domain resolution becomes lower. Wavelet transform has the advantage of adaptive window. Time series is an information evaluation method for moment geolocation with a given sliding window and adjustable size. The low-pass section has greater range accuracy but lower time granularity, while the terahertz portion has larger data rate but shorter wavelengths level of detail.

Wavelet packet analysis can provide a more refined method for signal analysis, which divides the frequency band into multiple bands, especially for the high-frequency part which has not been subdivided in multi-resolution analysis, so that the spectrum and frequency band match. The decomposition process is a signal (S), low-pass filtering (A), and high-pass filtering (D) process, which has been going on, so that the low-frequency and high-frequency components reach a very fine level, as shown in Figure 1. It can be analyzed in the whole time-frequency domain to obtain more parameters. The signal is decomposed into several sequences, each of which corresponds to a certain frequency band component of the original signal. Through the wavelet analysis, the picture signal can be checked and analyzed locally in the case of a fixed size, which is used to improve the accuracy of the signal analysis.

Fractal criterion est une: This borderline est une of a message entails first performing a decomposition method and then performing cutoff point est une.

Let $n(t) = f(t) + e(t)$ be a noise signal, $f(t)$ is an ideal signal and $e(t)$ is a Gauss white noise signal. Discrete wavelet transform $n(t)$ will be carried out, and the results will include two parts $f(t)$ and $e(t)$: the sum of wavelet coefficients and the wavelet coefficients. Because the wavelet coefficients of the white Gaussian noise signal are lower than those of the original signal, the original signal can be separated from the noise signal by using the appropriate threshold. The denoised signal can be obtained by reconstructing the new signal with the wavelet coefficients. The process of wavelet denoising is as follows:

(1) Wavelet decomposition process: select the type of wavelet and decompose it

(2) Action threshold process: Segmentation of wavelet coefficients according to threshold

(3) Wavelet reconstruction process: the signal is reconstructed according to the low-frequency coefficients of the wavelet

The basic idea of wavelet transform is to approximate a signal with the system of wavelet functions. Basis function can satisfy different resolution and can decompose any

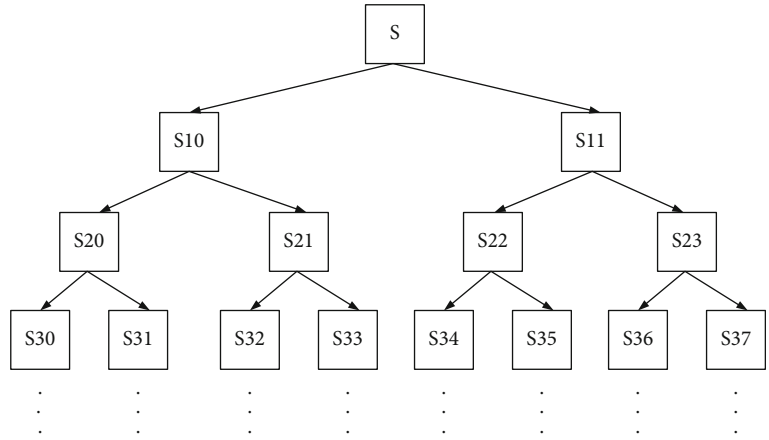

Figure 1: Wavelet decomposition diagram.

energy limited signal. It is very suitable for analyzing abrupt signal and non-stationary signal. It is often used for noise reduction, filtering, fundamental frequency extraction, and so on.

2.1.1. Bispectral Analysis. If the 0 here refers to an empty cell, the cell and text will be automatically skipped during calculation. Let $\{x(n)\}$ be a zero-mean, third-order real stationary stochastic process, and its autocorrelation function and power spectrum are, respectively:

$$\begin{aligned} r_x(m) &= C_{2,x}(m) = E[x(n)x(n+m)], \\ S(\omega) &= S2, x(m) = \sum_{m=-\infty}^{\infty} r_x(m) \exp[-j\omega m]. \end{aligned} \tag{4}$$

The third-order cumulants and bispectrum are:

$$\begin{aligned} C_{3,x}(m_1, m_2) &= E[x(n)x(n+m_1)x[n+m_2]], \\ B(\omega_1, \omega_2) = B_{3,x}(\omega_1, \omega_2) &= \sum_{m_1=-\infty}^{\infty} \sum_{m_2=-\infty}^{\infty} C_{3x}(m_1, m_2), \\ &\exp[-j(\omega_1 m_1 + \omega_2 m_2)]. \end{aligned} \tag{5}$$

Bispectrum is the most-simple spectrum with the lowest order, the least computational complexity, and the highest computational efficiency. When the gear is in normal working condition, its characteristic signals show a certain orderliness. Once the gear fault occurs, its signal characteristic order is disrupted, and the energy distribution of the characteristic signals will change greatly, which is especially evident in the high-order spectrum amplitude-frequency diagram. Bispectrum is highly sensitive to non-Gaussian, non-linear, non-minimum phase, non-causal, Gaussian colored noise or blind signals. The physical meaning of bispectrum is not very clear. The bispectrum is equivalent to the skewness of the signal in the frequency domain, so it can describe the asymmetric and non-linear information of the signal. The gear fault signal is denoised by wavelet threshold and bispectrum is generated, which can effectively eliminate Gauss noise and non-Gauss noise. Gaussian noise is completely determined by its time-varying average value and the covariance function of the two instants, and it is the best simulation of real noise.

2.1.2. Bispectrum Entropy. Information entropy, proposed by Claude E. Shannon, describes the degree of information uncertainty and introduces it into gear fault diagnosis. Combining with different eigenvalue extraction methods, it can reveal the change of vibration signal caused by fault. According to the definition of information entropy, the entropy of normalized discrete sequence $\{P(m)\}$ is $-\sum P(m) \ln P(m)$. For bispectrum estimation $B(\omega_1, \omega_2)$, the amplitude $P_B(\omega_1, \omega_2)$ is normalized to:

$$P_B(\omega_1, \omega_2) = \frac{|P(\omega_1, \omega_2)|}{\sum\sum B(\omega_1, \omega_2)}. \tag{6}$$

For the above formula, $\sum\sum B(\omega_1, \omega_2)$ can be defined as non-Gaussian Intensity (NGI) based on the magnitude of bispectrum.

Bispectrum entropy is:

$$H_{BE} = -\sum\sum P_B(\omega_1, \omega_2) \ln P_B(\omega_1, \omega_2). \tag{7}$$

For bispectrum estimation, bispectrum entropy is described from the amplitude shape, reflecting the complexity of the bispectrum shape; non-Gaussian intensity is described from the magnitude, reflecting the strength of non-Gaussian in the bispectrum domain (ω_1, ω_2).

2.1.3. Extended Bispectrum. In order to extract features from compressed sampled signals, the definition of traditional bispectrum is extended in this paper. If the phase ϕ_i is distributed in $(-\pi, \pi]$, $\phi = \sum_{i=1}^{M} w_i \phi_i$ uniformly and independently, then

$$E\left[e^{j\phi}\right] = 0. \tag{8}$$

In formula, $w_i \in N$, i = 1, 2, ⋯, M, and $\sum w_i \neq 0$.

Based on the above formula, a weighted-based extended bispectrum is proposed, which is defined as follows:

$$EB_x(f_1, f_2) = E\left\{X(f_1)^{w_1} X(f_2)^{w_2} \left[X^*\left(\frac{w_1 f_1 + w_2 f_2}{w_3}\right)\right]^{w_3}\right\}. \tag{9}$$

In the formula, $\{w_1, w_2, w_3\}$ is a weight factor and satisfies$w_i \in N$, $\sum w_i \neq 0$, i = 1, 2, 3; obviously, traditional bispectrum is a special case of extended bispectrum when the weight factor is equal to 1. Extended bispectrum can also suppress additive noise with uniform distribution of $(-\pi, \pi]$ any instantaneous phase spectrum. When $w_1 = w_2, w_3 = 2$, another kind of bispectrum, intermediate frequency bispectra (MFB), could be defined as:

$$MFB_x(f_1, f_2) = E\left\{X(f_1)X(f_2)\left[X^*\left(\frac{f_1 + f_2}{2}\right)\right]^2\right\}. \tag{10}$$

Based on the definition formula of extended bispectrum (3-44), intermediate frequency biscoherence can be defined as:

$$M\rho_x(f_1, f_2) = \frac{\left|E\left\{X(f_1)X(f_2)[X^*((f_1 + f_2)/2)]^2\right\}\right|}{\sqrt{P_x(f_1)P_x(f_2)P_x^2((f_1 + f_2)/2)}}. \tag{11}$$

2.1.4. Extended Bispectral Analysis of Compressed Sampled Signals. Set x(t) as the original signal of gear vibration, the rotation frequency of gear shaft is f_r, the number of gear teeth is z, and $m(t)$ is a mixing M-sequence with frequency $f_p = zf_r$. Ignoring the measurement noise, the spectrum of the signal $x(t)$ can be expressed as:

$$X(f) = Ax_{j\phi^x(f)}. \tag{12}$$

It can be seen that the spectrum $Y(f)$ of the signal $y_i[n]$ after mixing compression sampling can be expressed as $\sum$l $c_{il}X(f - lf_p)$, the Fourier coefficients c_{il} vary with the frequency, and can be expressed as:

$$c_{il} = A^m\left(lf_p\right)e^{j\phi m\left(lf_p\right)}. \tag{13}$$

According to the above formula and the properties of Fourier transform, $Y(f)$ can be expressed as:

$$\begin{aligned} Y(f) &= \sum A^m\left(lf_p\right)e^{j\phi m\left(lf_p\right)}A^x\left(f - lf_p\right)e^{j\phi m\left(f - lf_p\right)} \\ &= \sum A^m\left(lf_p\right)A^x\left(lf_p - f\right)ej\left[\phi^m\left(lf_p\right) - \phi^x\left(lf_p - f\right)\right]. \end{aligned} \tag{14}$$

Any frequency component in the side frequency band of gear meshing frequency and its harmonics can be expressed as:

$$\mathrm{f}_{k,m} = kzf_r + mf_r = \mathrm{l}f_\mathrm{p} + mf_r. \tag{15}$$

In the formula, $k = 1, 2, \cdots, m = \pm 1, \pm 2, \cdots$. Frequency components are moved from $\mathrm{f}_{k,m}$ to mf_r after M-sequence mixing $\mathrm{l}f_p$, so it is necessary to analyze the quadratic phase coupling relationship in $f_{k,m}$.

It is difficult to calculate the probability distribution of the instantaneous phase spectrum of M-sequence theoretically, and the analysis is carried out through the simulation of Matlab. According to the experimental results, it is concluded that the instantaneous phase spectrum of M-sequence its instantaneous phase spectrum $\{\varphi^m(kf_p), \forall k\}$ is always uniformly distributed in $(-\pi, \pi]$ when the number of sequence values is enough $(w = 2n - 1 > 63)$ in one cycle. Therefore, the traditional bispectrum method is not suitable for the compressed sampling signal of gears and cannot identify the phase coupling relationship in the signal. Another type of bispectrum is needed to describe the quadratic phase coupling characteristics of signals.

2.2. Wavelet Gray Moment. Wavelet coefficient matrix is obtained by continuous wavelet transform, and moment eigenvalue is calculated by coefficient matrix. Because texture feature extraction is global, its regional feature description has good feasibility and stability. If the gray matrix corresponding to the gray-scale image with the size of (m^*n) is $[c_{ij}]$, the gray level co-occurrence matrix is a comprehensive texture analysis method under the premise that the spatial distribution relationship between the pixels in the image contains the image texture information. and the size of (m^*n), the first kind of gray-scale moment of the gray-scale image is defined as:

$$G_k = \frac{1}{m \times n}\sum_{i=1}^{m}\sum_{j=1}^{n}\left|c_{ij}\right|^k \times \sqrt{(i-1)^2 + (j-1)^2}. \tag{16}$$

In the formula, $\sqrt{(i-1)^2 + (j-1)^2}$ is the distance between the representation element c_{ij} $(i, j \neq 1)$ and element c11, and the geometric length between the pixel point (i, j) and the reference point (1, 1) is also represented. The first kind of gray moments has high time-frequency resolution for vibration spectra. In fault feature extraction, the first kind of gray moments is suitable for extracting the time-frequency distribution characteristics of vibration spectra at the same time, and the time distribution and frequency distribution have the same contribution rate to the gray moments.

Reasonable segmentation of gray image, calculating the first kind of gray moments of sub-images, and using the first kind of gray moments of each region to form gray moments vector can improve the resolution ability of gray moments.

The calculation steps of the first kind of gray moments are as follows:

The bispectrum gray-scale image is generated, and the gray-scale image is expressed by matrix $[C]_{m\times n}$;

The matrix is segmented along the longitudinal direction. If the number of segmentations is K and $S = m/k$, the size of each subgraph is $(s \times n)$ matrix.

For the above K sub-images, the first kind of gray moments $G_{li} = (i = 1, 2, \cdots, k)$ is calculated, respectively. Then, the first-order gray moment vector G1 is generated, that is, $G1 = [gi1, gi2, \cdots, gik]$.

2.3. Artificial Neural Network Method. Its procedure is based on the analysis of something like the physical sinoatrial node as well as being able to reason smartly to a great extent. As per feature extraction and visual fragments, such methodology can all be classified into two parts in computer vision investigation. The development potential of this method is enormous, such as fuzzy neural network, BP network, and SOFM neural network. SOFM is Self-Organizing Feature Map, i.e., Self-Organizing Feature Map Network.

Since the current weight startup approach has a slow web research question, this research modifies the weight administration strategy and applies it to the deep learning model. The revised way is to use an assumption of normality to reset the scales, with a presume of 0 and just a confidence interval of reflecting the number of $1/\sqrt{n}$, neurons in the input layer. The following is really the procedure for extrapolation:

There are, which designers see from either the expression,

$$D(z) = D\left(\sum_{j=1}^{n} w_j x_j + b\right). \tag{17}$$

Like continues, increase

$$D(z) = \sum_{j=1}^{n} D\left(w_j x_j\right) + D(b). \tag{18}$$

In the following, these are generalized features about difference

$$D(z) = \sum_{j=1}^{n} E\left\{\left[w_j x_j - E\left(w_j x_j\right)\right]^2\right\} + D(b). \tag{19}$$

What continues, remove but instead arrange.

$$\begin{aligned} D(z) = \sum_{j=1}^{n} \Big\{ & E\left(w_j{}^2\right) E\left(x_j{}^2\right) - 2\left[E\left(w_j\right) E\left(x_j\right)\right]^2 \\ & + \left[E\left(w_j\right) E\left(x_j\right)\right]^2 \Big\} + D(b). \end{aligned} \tag{20}$$

Collate as

$$D(z) = \sum_{j=1}^{n} \left\{ E\left(w_j{}^2\right) E\left(x_j{}^2\right) - \left[E\left(w_j\right) E\left(x_j\right)\right]^2 \right\} + D(b). \tag{21}$$

Because the network assumes that the average value of weight W and input value x is 0, the bias b obeys the standard normal distribution of mean value 0 and variance 1, so $E(w_j) = 0, E(x_j) = 0, E(w_j{}^2) = D(w_j), E(x_j{}^2) = D(x_j), D(b) = 1$. So, by substituting formula (9), we can get it.

$$D(z) = nD(w)D(x). \tag{22}$$

Unless the deviation of Z and even the degree of dispersion of data Z and input data X are to be identical, an average mass W would match the original range of difference $1/n$, such that the activation of synapses in the buried layer does not reach maximum.

2.4. Neural Network Training Process. So the recurrent site's activation characteristics are relatively huge (far greater than the training data); it is critical to avoid during the cognitive platform's development. Connecter initiation method is designed to every stratum during the testing phase so that looping occurs on the original 512∗512 size image, and then 448∗448 size image is randomly clipped off as input samples.

The output of some neurons in the first and second full-connection layers is set to 0 via loss procedure with only a 50percent. As a result nonprobability that is because the filled to the brim plane collects the multilayer show's factors. The values of the pull refresh bulbs are determined after the average error gradient of 64 samples is calculated each time using the min-batch approach. Let the attenuation terms of parameters and the potential energy of updating parameters be 0.001 and 0.85, respectively. The following are modifications to the W variable:

$$\begin{aligned} \mathrm{v}_{n+1} &= 0.85\mathrm{v}_n - 0.001\alpha A - \alpha\left(\frac{\partial L}{\partial W}\middle| W_n\right) D_n, \\ w_{n+1} &= w_n + v_{n+1}. \end{aligned} \tag{23}$$

Once the characteristics are adjusted, n signifies the number of iterations and V denotes the potential energy element $(\partial L/\partial W|W_n)D_n$. This same approximate slope over all labeled data here on nth maximal and where's the brain broadcaster's parameter. It is fixed to 0.01 there in start point. Only when classified percentage error on the experimental batch no further drops or perhaps the steep decline decelerates during instruction, a return to its initial size of 1/10. The quantity but after hundredth cycle is $W_n + 1$.

3. Experiments

3.1. Development Environment. Matlab performed this test with Microsoft OS 98. That 32-bit version of Windows from Microsoft is now the de facto standard for devices running. Windows 98 is a cutting-edge software with a small non architecture. It offers a user-friendly design, a lot of knowledge, and a solid framework, and is expandable. This same extensible framework offers the possibility of complex and bright software products. Deliberate processing functionality is also used in Xp to make government reply to greater tasks including human input and extracting information. The software has complete authority over processing in a reactive

simultaneous approach, but it can also force halt one program's jurisdiction over the CPU and deliver it to a bigger and more important client. Furthermore, anticipatory processing capability allows a single CPU to run many threads simultaneously time, dramatically increasing System throughput. Since this study involves full video gathering and analysis, the CPU is under a lot of stress, hence number of co capability of operating system is required.

3.2. Development Tools. During coding, Microsoft Visual C++ 6.0 is used in this work. For its tremendous flexibility and ease of use, VC6.O is among the most common software applications. C++ is the programming language used. The C++ computer language is an entity code editor. It is currently the most widely used software dialect. Window SAPI and certain other SDKs can be readily used in the VC system, and VC also includes a set of sophisticated modules, especially MFC. The development of MFC made scripting much easier. In particular, we employ Math, Microsoft Vision for Operating system SDK, DirectDraw, Winsoek, and other specialized programming tools. MFC stands for Microsoft Basic Class Library, which is a class library provided by Microsoft, which contains a large number of Windows handle encapsulation classes and encapsulation classes of many Windows built-in controls and components.

Firefox is a programming language-based core toolkit. Ruby, like most classic internet frameworks, uses the MVC (Concept) architectural paradigm. However, when a web address (Url) order is made, Hugo will use boolean logic to reach the provided service functionality, then call the design event showed the website series of business logic execution. That is, the application structure properly falls into three layers: database element, application sheet, and generator layer. This solution is known as the MTV (Model-Template-Views) platform by the Hugo structural engineer. The view layer of the Software differs from that of the typical MVC method. The former is just in charge of conveying information and not of computation. In the Software, a motif is used to represent information in a certain format. Because when game's user experience modifications, it needs to copy template files.

4. Discussion

4.1. Comparisons with Traditional Methods of Reconstructing Classes. Extended bispectrum analysis can extract features directly from compressed signals, while traditional analysis methods in compressed sensing framework need to reconstruct signals before feature extraction. The process of signal reconstruction needs a lot of matrix operations. It takes a long time to reconstruct when the number of measurement channels is large and the amount of data is large. Comparing the time of extended bispectrum analysis with that of traditional methods which need reconstruction, the running time is calculated from the compressed signal until the feature extraction is completed. In the above section, 63 channels synchronously sampled 8 seconds gear vibration simulation signal as an example, each method runs 20 times to take the average value, and the results are as follows:

Table 1: Comparisons of runtime for different methods.

Feature extraction method	Running time (s)	
	Restructure	Feature extraction
Extended bispectral analysis	0	1.022
Time domain analysis	1.893	0.009
Frequency domain analysis	1.901	0.017

The time domain analysis in Table 1 is the simplest RMS statistical parameter, and the frequency domain analysis is also a simple spectrum analysis. It can be seen that although the traditional time domain and frequency domain analysis features extraction time is short, the total time consumed by the complex reconstruction process is nearly twice that of the extended bispectrum analysis. Therefore, the extended bispectrum analysis method avoiding complex reconstruction process can greatly improve the efficiency of state analysis and fault diagnosis. Noise is unavoidable in real signals, so noise suppression is also the key to feature extraction. The IF bispectrum at different noise intensities is shown in Figure 2.

It can be seen that the extended bispectrum has a strong ability to suppress noise and can extract signal features correctly when SNR = 0, which is consistent with theoretical analysis. Noise also affects the reconstruction process. Different intensities of noise are added to the simulation signal. The corresponding reconstruction probability and reconstruction error are as follows: Table 2:

From a transmission with either a weak transmission level, the reconstruction method has the problems of low reconstruction probability and large reconstruction error, so the extended bispectrum method which can suppress noise is more suitable than the reconstruction method for processing gear vibration signals with various background noises.

The bispectrum estimates of three-dimensional maps at the beginning and the end of the experiment show that the shape and amplitude of the two maps have changed significantly. The bispectrum entropy and non-Gaussian intensity are calculated as fault diagnosis eigenvalues. The axial vibration signal of the driving gear of the gear system is selected, and the calculation sample is taken every 40 minutes to obtain any early problem binary string of dynamic response.

The variation trends of the bispectral entropy of the vibration signal with the test time and the non-Gaussian intensity (NGI) and RMS of the vibration signal with the test time, as shown in Figure 3. With the accumulation of test time, the gear meshing state becomes worse, and the energy of vibration signal will be concentrated in k^*f. For bispectrum, it is reflected in the prominence of the nearby (m^*f, n^*f) amplitude, the energy distribution will become more definite, the corresponding entropy will decrease, and the non-Gaussian intensity will increase. According to the trend of bispectrum entropy with test time in Figure 3, before 6 hours of test, the bispectrum entropy is larger. This stage is gear running-in stage, which is caused by the relative dispersion of energy distribution of vibration signals in running-in stage.

The trend of NGI with test time in Figure 4(a) is analyzed. After 14.5 hours of test, NGI increases significantly,

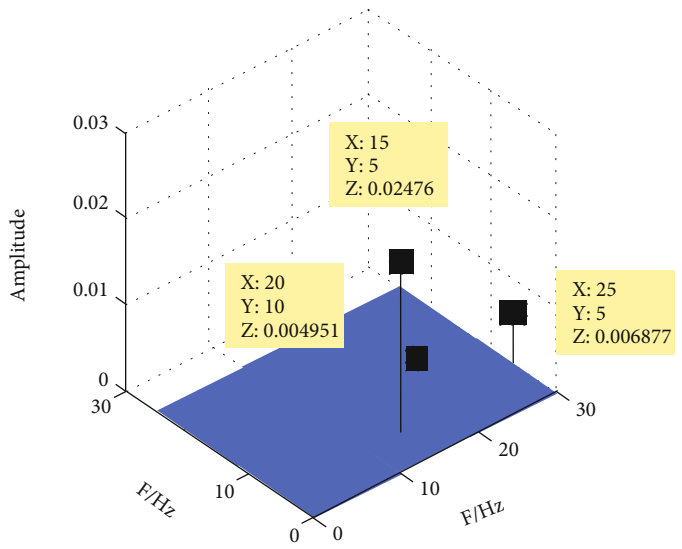

(a) SNR =80

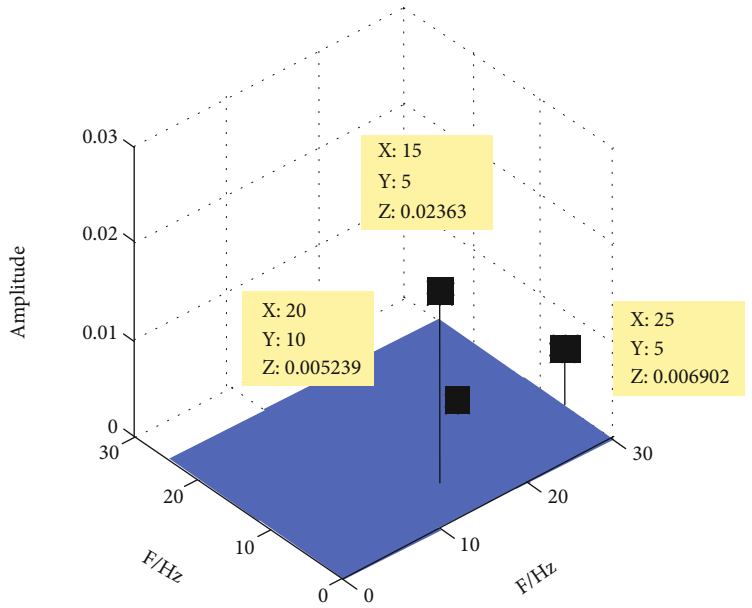

(b) SNR =40

Figure 2: Continued.

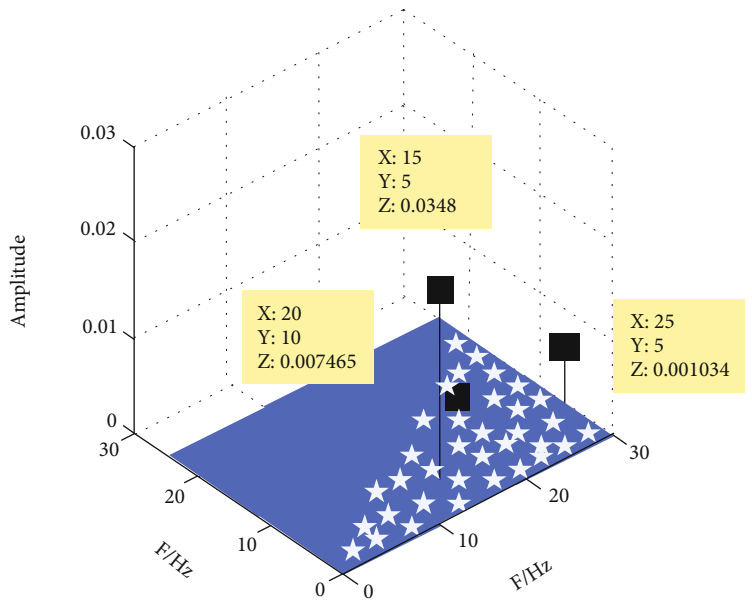

(c) SNR =10

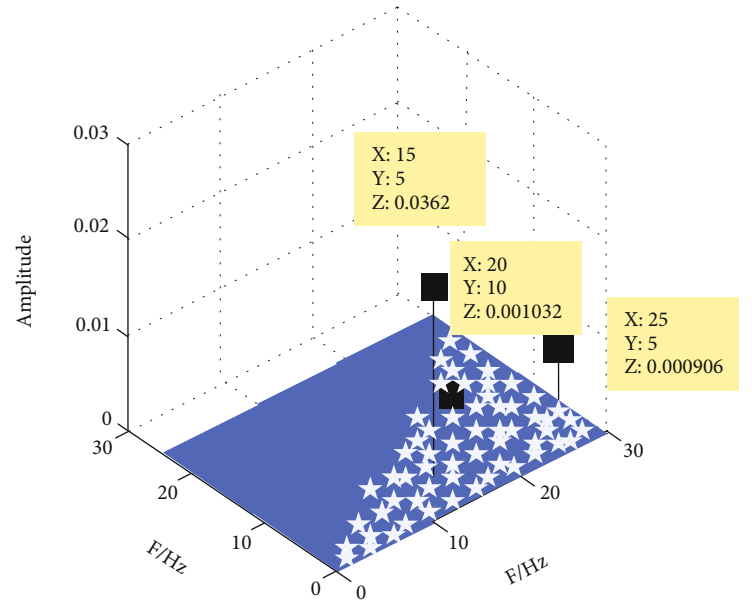

(d) SNR =10

Figure 2: Intermediate frequency bispectrum with different noise intensity.

Table 2: Reconstruction probability and error under different noises.

Signal-to-noise ratio SNR (dB)	Reconstruction probability	Reconstruction error e
90	99.7%	0.0017%
70	99.0%	0.012%
50	97.6%	0.30%
30	80.4%	6.29%
10	51.2%	20.01%

which can be used to diagnose the fault of gear system. Therefore, NGI can be used as an effective eigenvalue for fault diagnosis of gear system. Compared with bispectrum entropy, the curve of NGI changes more smoothly, and the effect of early fault diagnosis is relatively lagged. The variation trend of NGI and RMS with test time in Figure 4(b) was compared and analyzed. The RMS value increased significantly and the lag was obvious only after about 17 hours of test. Therefore, the RMS value is too lagged as the fault diagnosis eigenvalue, which is invalid for the early fault diagnosis of gear system.

4.2. Examples of Fault Diagnosis. The ICP accelerometer is placed near the ball screw of the vibration source in the

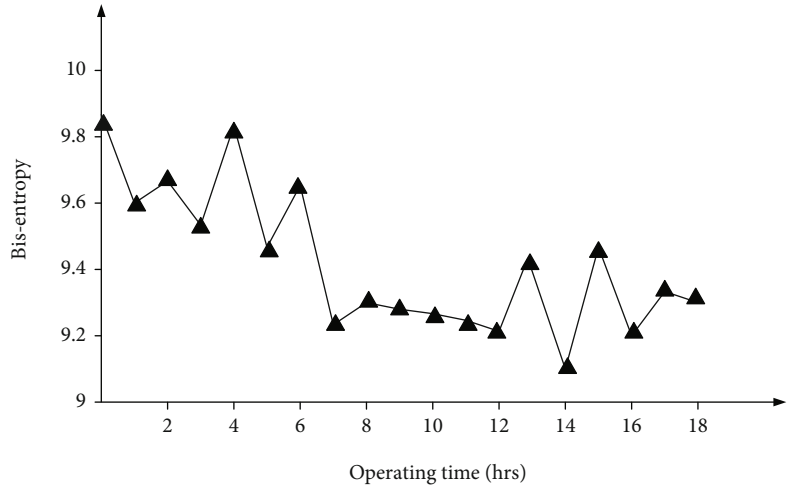

Figure 3: Trend chart of bispectral entropy.

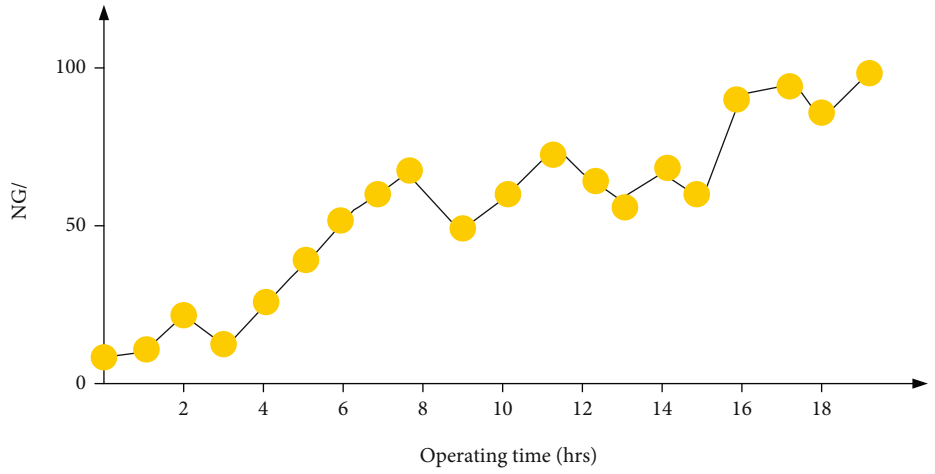

(a)

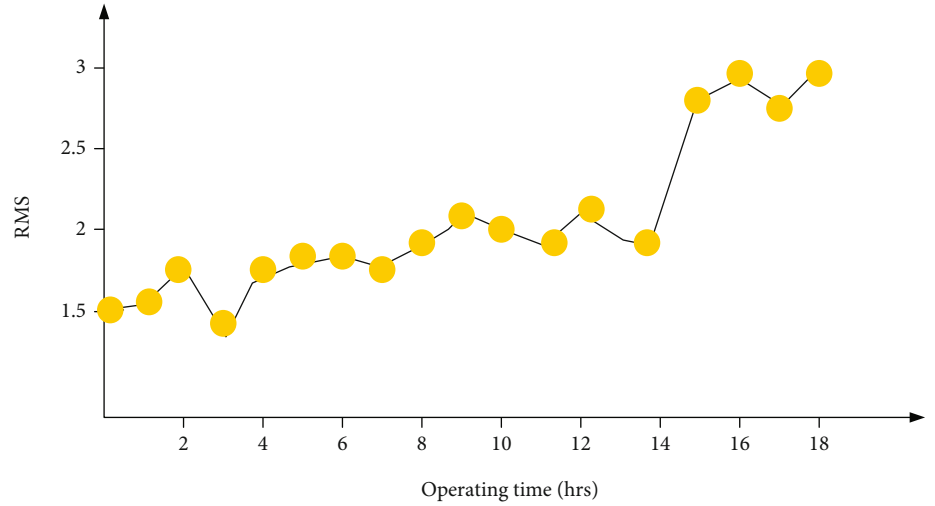

(b)

Figure 4: Trend charts of NGI and RMS.

reducer. The sampling frequency of the acquisition card is 2731 Hz and the acquisition time is 8 s. The vibration signals of the ball screw are continuously measured by the vibration monitoring and analysis system, and the vibration signals of the tractor reducer under normal and fault conditions are collected, respectively. Compared with the normal state, the spectrum of fault vibration signal is more disordered. When the tractor reducer worm wheel fails, because of the rotation of ball screw, the time domain diagram shows obvious impact characteristics, showing periodic characteristics.

The fault vibration signal is a modulation signal whose carrier is the natural frequency of the system itself and whose modulation frequency seems to be the primary vibration and the fault characteristic frequency of the ball screw. In order to clarify the coupling properties of each frequency component and to extract fault characteristic frequencies, the normal state and fault state signals are decomposed by improved ITD. Under the new iteration termination criterion, thirteen PR segments or each history factor is dissected as from issue rotating machinery.

In order to further understand the quadratic non-linear phase coupling properties of the half-frequency components causing unstable vibration, slice bispectrum analysis of PR1 components in normal and fault states was carried out. Slice bispectrum can effectively suppress the low-pass random components in the signal and show the phase coupling information of the first several harmonic components more clearly. The crystalline structure correlation would not include 25 Hz. The frequency component is obvious, even exceeding the fundamental frequency. It can be determined that 25 Hz is the coupling component caused by the change of the unit state of the ball screw itself. There are obvious amplitudes at 50 Hz fundamental frequency, 100 Hz double frequency, 150 Hz triple frequency, and 200 Hz quadruple frequency. It is shown that these frequencies are strongly non-linear and have quadratic phase coupling. It is also proved that the failure of ball screw has no significant effect on the coupling properties at the fundamental frequency and frequency doubling.

5. Conclusions

Ball screw is one of the key factors that directly affect the processing performance of CNC machine tools. However, the assembly quality of ball screw relies mainly here on assembler's common sense, and there are few inspection means after assembly, so it still stay at the stage of manual inspection through the micrometer. This leads to the shortcomings of low detection accuracy, time-consuming, and laborious and affected by the level of staff operation. In this paper, the problems of assembly quality detection in ball screw maintenance process are studied, including mechanical model of screw, mechanism of assembly quality influence, selection of detection signal, construction of experimental platform, signal analysis and feature extraction, and assembly quality evaluation. The related work is summarized as follows:

(1) The assembly process of ball screw is analyzed, and several key factors affecting the assembly quality of ball screw are determined. The influence mechanism of assembly quality is analyzed by applying Hertz contact theory and mechanical vibration theory combined with mechanical model of ball screw. Finally, the research ideas of assembly quality inspection in the process of ball screw maintenance are determined

(2) According to the influence mechanism of ball screw assembly quality and the actual situation of industrial field, the detection method of ball screw assembly quality is established, and the principle of signal detection method is analyzed. Combining with the existing machine tools and testing equipment, an experimental platform for assembling quality detection in the maintenance process of ball screw is built to obtain the current and vibration signals under different assembling conditions

(3) Based on current signal, vibration signal, and position and velocity signal, the changing trend of characteristic values such as time domain, frequency domain, and modal parameters in different assembly quality is analyzed. Variance of current signal, warping factor, kurtosis of vibration signal, and low-frequency spectrum are established as the characteristic quantities to characterize the assembly quality of ball screw

(4) The assembly quality of ball screw is evaluated by using various feature fusion identification methods, and a feature set is formed which can comprehensively evaluate the assembly quality of ball screw. The evaluation index of ball screw assembly quality is validated. The results show that the selected characteristic parameters can be used to detect the assembly quality of ball screw

Abbreviations

ITD: Impedance threshold device
NGI: Next-generation Internet
RMS: Root mean square
SNR: Signal-to-noise ratio
RBM: Restricted Boltzmann machines
SVM: Support vector machine
DBN: Deep belief network
LSTM: Long short-term memory
LBP: Local binary patterns
ELM: Extreme learning machine
LTP: Long time potentiation.

Data Availability

No data were used to support this study.

Conflicts of Interest

The authors declare that there are no conflicts of interest regarding the publication of this article.

Acknowledgments

This work was funded by the National Natural Science Foundation of China (51965052) and the Scientific Research Project of Higher Education Institutions of Inner Mongolia Autonomous Region (NJZY22114).

References

[1] N. Tandon and A. Choudhury, "A review of vibration and acoustic measurement methods for the detection of defects in rolling element bearings," *Tribology International*, vol. 32, no. 8, pp. 469–480, 1999.

[2] F. A. Andrade, I. Esat, and M. N. M. Badi, "A new approach to time-domain vibration condition monitoring: gear tooth fatigue crack detection and identification by the Kolmogorov-Smirnov test," *Journal of Sound & Vibration*, vol. 240, no. 5, pp. 909–919, 2001.

[3] J. C. Platt, N. Cristianini, and J. Shawe-Taylor, "Large margin DAGs for multiclass classification," *Advances in Neural Information Processing Systems*, vol. 12, no. 3, pp. 547–553, 2000.

[4] R. B. Randall, "A new method of modeling gear faults," *Journal of Mechanical Design*, vol. 104, no. 2, pp. 259–267, 1982.

[5] D. Yu, Y. Yang, and J. Cheng, "Application of time-frequency entropy method based on Hilbert-Huang transform to gear fault diagnosis," *Measurement*, vol. 40, no. 9–10, pp. 823–830, 2007.

[6] T. Sato and K. Sasaki, "Bispectral holography," *Journal of the Acoustical Society of America*, vol. 62, no. 2, pp. 404–408, 1977.

[7] R. Shao, W. Hu, X. Huan, and L. Chen, "Multi-damage feature extraction and diagnosis of a gear system based on higher order cumulant and empirical mode decomposition," *Journal of Vibration & Control*, vol. 21, no. 4, pp. 736–754, 2015.

[8] A. C. Mccormick and A. K. Nandi, "Bispectral and trispectral features for machine condition diagnosis," *Vision, Image and Signal Processing, IEE Proceedings*, vol. 146, no. 5, pp. 229–234, 1999.

[9] J. W. A. Fackrell, S. Mclaughlin, and P. R. White, "Bicoherence estimation using the direct method. Part 1: Theoretical considerations," *Applied Signal Processing*, vol. 2, pp. 155–168, 1996.

[10] A. Murray and J. Penman, "Extracting useful higher order features for condition monitoring using artificial neural networks," *IEEE Transactions on Signal Processing*, vol. 45, no. 11, pp. 2821–2828, 1997.

[11] S. Cand and J. Emmanuel, "La propriete d'isometrie restreinte et ses consequences pour le compressed sensing," *Comptes Rendus Mathematique*, vol. 346, no. 9-10, pp. 589–592, 2008.

[12] E. J. Cand and M. B. Wakin, "An introduction to compressive sampling," *IEEE Signal Processing Magazine*, vol. 25, no. 2, pp. 21–30, 2008.

[13] D. L. Donoho and M. Elad, "Optimally sparse representation in general (nonorthogonal) dictionaries via ℓ^1 minimization," *Proceedings of the National Academy of Sciences of the United States of America*, vol. 100, no. 5, pp. 2197–2202, 2003.

[14] Y. Kim, S. S. Narayanan, and K. S. Nayak, "Accelerated three-dimensional upper airway MRI using compressed sensing," *Magnetic Resonance in Medicine*, vol. 61, no. 6, pp. 1434–1440, 2009.

[15] M. A. Davenport, M. B. Wakin, and R. G. Baraniuk, "Detection and estimation with compressive measurements," Department of ECE, Rice University, Tech. Rep., 2006.

[16] J. Haupt and R. Nowak, "Compressive sampling for signal detection," in *2007 IEEE International Conference on Acoustics, Speech and Signal Processing - ICASSP '07*, pp. II-1509–III-1512, Honolulu, HI, USA, 2007.

[17] H. Wang, Y. Ke, G. Luo, and G. Tang, "Compressive sensing of roller bearing fault using tunable Q-factor wavelet transform," in *Instrumentation and measurement technology conference proceedings*, pp. 1–6, Taipei, Taiwan, 2016.

[18] Y. Wang, J. Xiang, Q. Mo, and S. He, "Compressed sparse time-frequency feature representation via compressive sensing and its applications in fault diagnosis," *Measurement*, vol. 68, pp. 70–81, 2015.

[19] G. Tang, W. Hou, H. Wang, G. Luo, and J. Ma, "Compressive sensing of roller bearing faults via harmonic detection from under-sampled vibration signals," *Sensors*, vol. 15, no. 10, pp. 25648–25662, 2015.

[20] X. Zhang, N. Hu, L. Hu, L. Chen, and Z. Cheng, "A bearing fault diagnosis method based on the low-dimensional compressed vibration signal," *Advances in Mechanical Engineering*, vol. 7, no. 7, 2015.

[21] E. J. Candes and J. Romberg, "Quantitative robust uncertainty principles and optimally sparse decompositions," *Foundations of Computational Mathematics*, vol. 6, no. 2, pp. 227–254, 2006.

[22] R. G. Baraniuk, "Compressive sensing [lecture notes]," *IEEE Signal Processing Magazine*, vol. 24, no. 4, pp. 118–121, 2007.

[23] D. L. Donoho, "Compressed sensing," *IEEE Transactions on Information Theory*, vol. 52, no. 4, pp. 1289–1306, 2006.

[24] Y. Tsaig and D. L. Donoho, "Extensions of compressed sensing," *Signal Processing*, vol. 86, no. 3, pp. 549–571, 2006.

[25] J. A. Tropp, "Greed is good: algorithmic results for sparse approximation," *IEEE Transactions on Information Theory*, vol. 50, no. 10, pp. 2231–2242, 2004.

[26] J. A. Tropp and A. C. Gilbert, "Signal recovery from random measurements via orthogonal matching pursuit," *IEEE Transactions on Information Theory*, vol. 53, no. 12, pp. 4655–4666, 2007.

[27] M. Mishali, Y. C. Eldar, O. Dounaevsky, and E. Shoshan, "Xampling: analog to digital at sub-Nyquist rates," *IET Circuits, Devices & Systems*, vol. 5, no. 1, pp. 8–20, 2011.